Measurements and Numerical Modeling of Wind Driven Circulation and Pollutant Transport

ASU İNAN[1], LALE BALAS[2], MURAT CETİN[3]
[1] Enviromental and Technical Research of Accidents Department
[2,3] Civil Engineering Department
Gazi University
Gazi University Institute of Science & Technology 06570 Maltepe/ Ankara TURKEY
[1] asuinan@gazi.edu.tr, http://www.fbe.gazi.edu.tr/kazalar/English/asuinani.htm
[2] lalebal@gazi.edu.tr, http://www.mmf.gazi.edu.tr/insaat/english/academicstaff/cv/lalebalasi.htm
[3] mcetin23@gmail.com

Abstract - Antalya Bay is located in the Mediterranean Sea of Turkish coasts. City of Antalya is one of the major tourism cities of Turkey with an increasing population. The sea outfall was constructed in the Antalya Bay. In this study, the currents and wind have been observed and measured. The wave height distribution, current pattern and pollutant concentration have been presented. Wind driven currents have been numerically modeled with the HYDROTAM 3 which is a powerfull tool to simulate hydrodynamics of a coastal area. The bacterial pollutant transport distribution due to the sea outfall of Antalya city was numerically modeled.

Key-words: Current, wave, pollutant, concentration, measurement, numerical modeling, Antalya Bay, sea outfall, coastal pollution, finite difference, finite element

1 Introduction

Antalya is located at the Mediterranean coast of Turkey in South Anatolia. The natural richness of Antalya has attracted many diverse civilizations over the centuries. The development of tourism, agriculture and agriculture based industry combined expanding domestic and foreign trade volumes ensures the growing importance of Antalya. Antalya is known as Turkish Riviera due to archaeological and natural riches.

The construction of the Antalya Sea Outfall was finalised in 1997. The length of the main pipeline in the sea of the sea outfall is 2600m and the length of diffusor crosssection is 315m.

An integrated water and wastewater project has been initiated in 1996 to protect groundwater resources and seawater quality in Antalya. The project includes wastewater collection, treatment and disposal by a long and deep sea outfall. A seawater quality monitoring program begun around the sea outfall in 1999. It comprised in situ measurement and lab analyses of the shore and offshore seawater quality parameters such as temperature, salinity, conductivity, dissolved oxygen, total and fecal coliforms [1]. Another important subject for Antalya Bay is estimation of bacterial inactivation variations due to Antalya sea outfall. Aral et al., studied on the estimation of T_{90} bacterial die-off rate values in the Antalya Bay in the seasons of winter and summer in 1993. They applied two different test method to get T_{90} values. These are tracer and plastic bag method [2]. The monitored degrees of vertical density strafication at the discharge point of sea outfall showed considerable temporal variations. The study of Yalcin and Muhammetoglu carried out to compute the levels of the discharged effluent dilutions due to bacterial inactivation around the sea outfall. The bacterial inactivation rate and the sea current speeds and directions are the

most important parameters of computations. According to the Turkish standarts, the value of T_{90} at the seasurface ranges from 1.5 to 5.0 hours depending on the seasons of the year [3].

The project called 'Investigation of Uncertainties in Predicting Bacterial Concentrations of Discharged Sewage from Deep Sea Outfalls When Submergence Occurs in Receiving Media' is a TUBITAK research project under incorporations of Akdeniz University, Gazi University and İstanbul Tchnical University. This project begun in the year of 2008. The aim of this project is to investigate the uncertainties associated with predicting bacterial concentrations from discharged sewage in the marine environment which exhibits density stratification. In order to achieve this aim, Antalya deep sea outfall is chosen to apply the study. First, the input parameters will be determined both in the field and in the lab for one year to investigate the temporal changes. In this respect, the vertical density stratification will be determined seasonally by measuring temperature and salinity around Antalya sea outfall. Bacterial inactivation values will be measured both in the lab and in the field. A three dimensional hydrodynamic model and discharge model will be applied to predict the current velocities and dilution values. The dilution values will be used directly to predict the bacterial concentrations around Antalya sea outfall. The predicted current velocities and bacterial concentrations will be calibrated and verified by using field measurements of current velocities and bacterial concentrations. Uncertainty analyses using Monte Carlo simulations will be used to investigate the uncertainties in predicting the coliform bacteria concentrations and to rank the input parameters according to their importance. Additionally, assessment of health risks to exposure to certain levels of bacterial coliform will be carried out. Alternative management scenarios to mitigate the adverse impacts of discharging sewage on the bacteriological water quality will be investigated. This gains importance as the region shows high tourism activity for which the quality of sea water is an essential parameter [4].

In this paper, a part of the project has been presented.

In this study, the current paths have been determined based on the measurements. The wave height distribution has been given. Currents and bacterial pollution due to sea outfall have been modeled numerically by HYDROTAM 3, respectively.

2 Field Study

The location of Antalya coastal region in Turkey has been shown in the Fig. 1.

Fig. 1: Map of Turkey [5]

Either Lagrangian method or Euler method have been used to determine current pattern of the coastal area. Lagrangian method was used for determination of the buoys dragging with the same velocity with currents. Euler method was used for the currents along depth in the same local point. Coastal currents were examined using GPS (Global Positioning System). The ultrasonic aquadoppler was selected as measurement aparatus for Euler method. The ultrasonic aquadoppler was installed in the exit of the diffusor. The buoys used in the field have been shown in the Fig. 2. Different sizes of the buoys are designed aiming the use of

buoys for different depths (85x85cm, 35x35 cm).

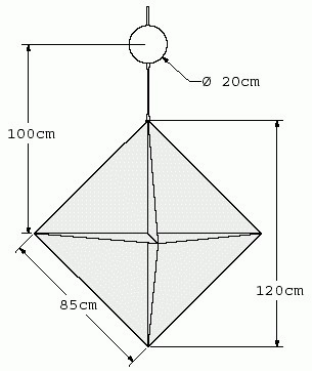

Fig. 2: The geometrical characteristics of a 85×85cm buoy

The monitored path lines of currents during the measurements for several depths have been shown in the Fig. 3 .

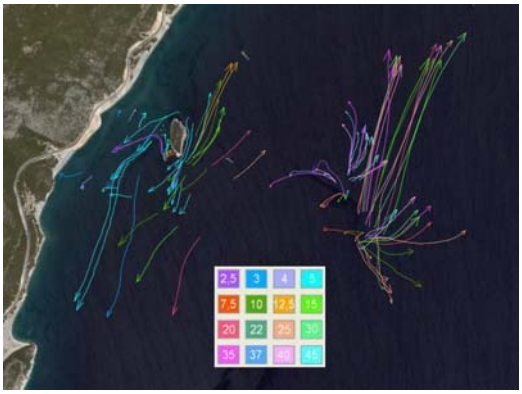

Fig. 3: The paths of the buoys in different depths during measurements (Depths are in meters)

The currents where the diffusor is located are generally move from south to north. It is observed that the current velocites change from 3cm/sec on the bottom to 17cm/sec at the surface. The currents in north and south of the island move in the NE and SW directions, respectively. A circulation region occurs between west and southwest of island. At the surrounds of the island, the current velocities are generally 21cm/sec at the surface and 2cm/sec on the bottom.

The currents were measured inbetween 24 and 29 September 2008. Second part of measurements were performed from 23 October 2008 to 27 October 2008. The data were surveyed from 07:20 to 17:20 in each day during field study. The wind rose has prepared for the wind data obtained during the field study. It is shown in The Figure 4. The histogram for wind data depending on the direction and velocity is given in the Fig. 5.

Prevailing wind during the field study is S and the most occurency of the wind velocities is in the range of 3-6m/sec as given in the wind rose and histogram in the Fig. 4 and Fig. 5.

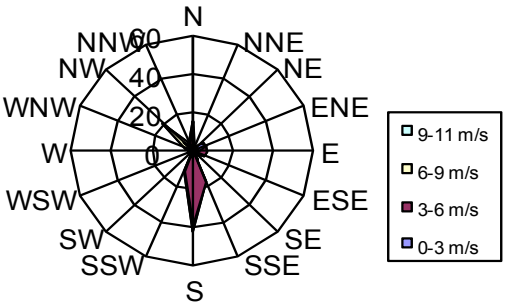

Fig. 4: Wind rose for the wind data during the field study

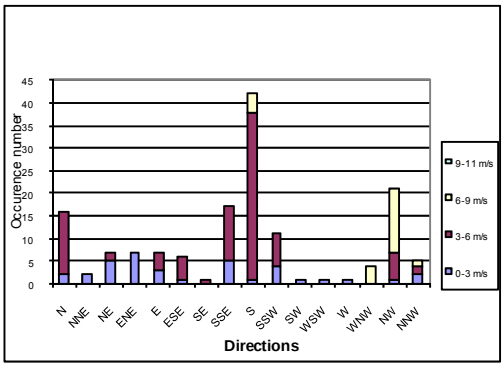

Fig. 5: Histogram of wind distribution depending on the directions

The annual wave rose for the coastal area has shown in Fig. 6. It is obtained from wind and deep water wave atlas for Turkish coast [6].

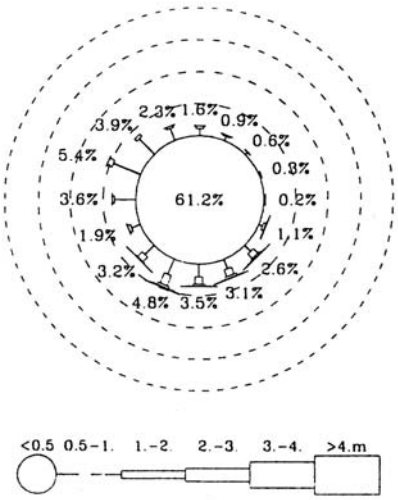

Fig 6. Annual wave rose [6]

3 Numerical Modeling

The studied coastal region is an important subject in the point of view of coastal engineering because of the Antalya sea outfall. Therefore the wave height distribution, current pattern and bacterial pollution due to the diffusor have been simulated numerically. The wave height has been calculated based on linear theory. HYDROTAM3 well known numerical tool has been applied to simulate 3D hydrodynamics of a coastal region.

3.1 Wave Height Distribution

Significant wave height and wave period have been obtained from the formulations given in SPM [7]. Used wind velocity to get significant wave height and wave period is 10m/sec. Deep water wave height is 3.61m and wave period is 10 sec. Applied wave incidence angle is zero because dominant wave direction is S. The wave heights have been calculated based on linear theory. The bathymetry of the coastal region has been shown in Fig. 7. The wave height distribution has been given in Fig. 8. Water depths and wave heights are in meters in Fig. 7 and in Fig. 8, respectively.

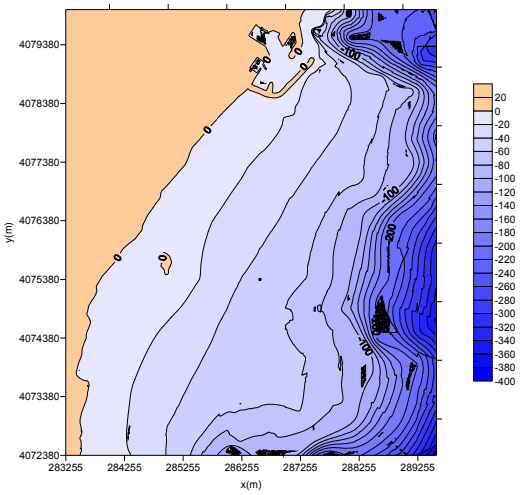

Fig. 7: Bathymetry of the coastal region

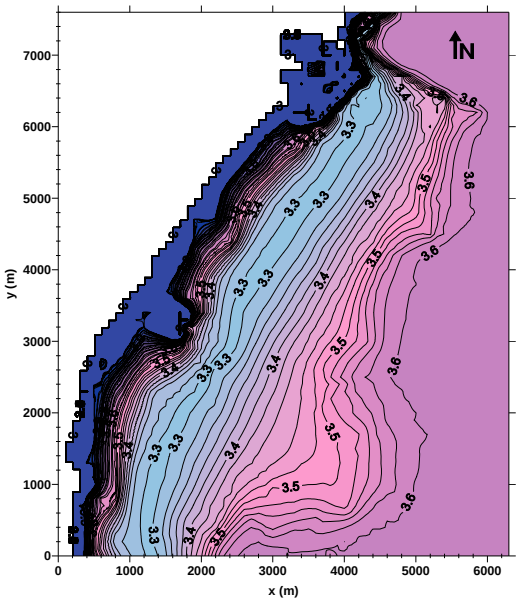

Fig. 8: Wave height distribution

3.2 Numerical Simulation of Currents and Pollution Distribution

The current pattern and concentration distrubution have been simulated with HYDROTAM 3.

HYDROTAM 3 is a three dimensional baroclinic numerical model which consist of hydrodynamic, transport and turbulence model components. It includes wind, tide or density induced currents, water levels, salinity and temperature variations, transport

of pollutants, forced flushing (sink or source induced currents) [8, 9].

In the hydrodynamic model component, the Navier- Stokes equations are solved with the hydrostatic pressure distribution assumption and Boussinesq approximation.

$$\frac{\partial u}{\partial x}+\frac{\partial v}{\partial y}+\frac{\partial w}{\partial z}=0 \tag{1}$$

$$\begin{aligned}&\frac{\partial u}{\partial t}+u\frac{\partial u}{\partial x}+v\frac{\partial u}{\partial y}+w\frac{\partial u}{\partial z}=\\&fv-\frac{1}{\rho_o}\frac{\partial p}{\partial x}+2\frac{\partial}{\partial x}(\nu_x\frac{\partial u}{\partial x})+\\&\frac{\partial}{\partial y}(\nu_y(\frac{\partial u}{\partial y}+\frac{\partial v}{\partial x}))\\&+\frac{\partial}{\partial z}(\nu_z(\frac{\partial u}{\partial z}+\frac{\partial w}{\partial x}))\end{aligned} \tag{2}$$

$$\begin{aligned}&\frac{\partial v}{\partial t}+u\frac{\partial v}{\partial x}+v\frac{\partial v}{\partial y}+w\frac{\partial v}{\partial z}=\\&-fu-\frac{1}{\rho_o}\frac{\partial p}{\partial y}+2\frac{\partial}{\partial y}(\nu_y\frac{\partial v}{\partial y})+\\&\frac{\partial}{\partial x}(\nu_x(\frac{\partial v}{\partial x}+\frac{\partial u}{\partial y}))+\frac{\partial}{\partial z}(\nu_z(\frac{\partial v}{\partial z}+\frac{\partial w}{\partial y}))\end{aligned} \tag{3}$$

$$\begin{aligned}&\frac{\partial w}{\partial t}+u\frac{\partial w}{\partial x}+v\frac{\partial w}{\partial y}+w\frac{\partial w}{\partial z}=\\&-\frac{1}{\rho_o}\frac{\partial p}{\partial z}-g+\frac{\partial}{\partial y}(\nu_h(\frac{\partial w}{\partial y}+\frac{\partial v}{\partial z}))+\\&\frac{\partial}{\partial x}(\nu_h(\frac{\partial w}{\partial x}+\frac{\partial u}{\partial z}))+\frac{\partial}{\partial z}(\nu_z\frac{\partial w}{\partial z})\end{aligned} \tag{4}$$

where, x and y are horizontal coordinates, z is vertical coordinate, t is time, u, v, w are velocity components and v_x, v_y, v_z:are eddy viscosities in x, y, z directions, respectively. f is Corriolis coefficient, ρ(x,y,z,t) is water density, ρ_o is reference density, g is gravitational acceleration and p is pressure.

The transport model component consist of the pollutant transport model and water temperature and salinity transport models. In this component, the three-dimensional convective diffusion equations are solved for each of the three turbulence and its rate of dissipation, which provides the variable vertical turbulent eddy viscocity. Horizontal eddy viscosity has been calculated by subgrid scale turbulence model and vertical eddy viscosity has been simulated by k-ε turbulence model [8, 9, 10].

Water density depends on temperature, salinity dominantly and pressure secondary. Average sea water density is 1.0276 g/cm^3. But when sea water density is compared with the other densities, it can be decided that three digits of this value is important. Therefore real water density ρ can be shown as sea water density σ_t [9].

$$\sigma_t=(\rho-1)\times 10^3 \tag{5}$$

Density is a function of salinity and temperature as shown in the formulation given below.

$$S=1{,}80655\ Cl \tag{6}$$

$$\begin{aligned}&\sigma_o=-6{,}9\times10^{-2}+1{,}4708\ Cl\\&-1{,}57\times10^{-3}\ Cl^2+3{,}98\times10^{-5}\ Cl^3\end{aligned} \tag{7}$$

$$\begin{aligned}&A_t=4{,}7867\times10^{-3}\ T-\\&9{,}8185\times10^{-5}\ T^2+1{,}0843\times10^{-6}\ T^3\end{aligned} \tag{8}$$

$$\begin{aligned}&B_t=1{,}803\times10^{-5}\ T-\\&8{,}146\times10^{-7}\ T^2+1{,}667\times10^{-8}\ T^3\end{aligned} \tag{9}$$

$$\Sigma_t=-(T-3{,}98)^2\frac{(T+283)}{(503{,}57(T+67{,}26))} \tag{10}$$

S is salinity (%), Cl is chlorine (gr/kg), T is temperature (^{o}C).

Temperature and salinity values must be computed in the nodal point to be able to calculate the density in each nodal point. Therefore three dimensional diffusion and convection equation (11) is solved.

$$\frac{\partial Q}{\partial t}+u\frac{\partial Q}{\partial x}+v\frac{\partial Q}{\partial y}+w\frac{\partial Q}{\partial z}= \frac{\partial}{\partial x}\left(D_x\frac{\partial Q}{\partial x}\right)+\frac{\partial}{\partial x}\left(D_y\frac{\partial Q}{\partial y}\right)+ \frac{\partial}{\partial z}\left(D_z\frac{\partial Q}{\partial z}\right) \quad (11)$$

Here, D_x, D_y ve D_z are turbulent diffusion coefficients in x, y, z directions, respectively. Q is water temperature and S is salinity.

The conservation equation of a pollutant constiuent given in (12) is used to observe the change of a pollutant.

$$\frac{\partial C}{\partial t}+u\frac{\partial C}{\partial x}+v\frac{\partial C}{\partial y}+w\frac{\partial C}{\partial z}= \frac{\partial}{\partial x}\left(D_x\frac{\partial C}{\partial x}\right)+\frac{\partial}{\partial x}\left(D_y\frac{\partial C}{\partial y}\right)+S_s \frac{\partial}{\partial z}\left(D_z\frac{\partial C}{\partial z}\right)+k_pC \quad (12)$$

Where, C is pollutant concentration, k_p is the decay rate of the pollutant D_x, D_y and D_z are turbulent diffusion coefficents in x, y, z, respectively.

Pollutant decay rate k_p is calculated with the term T_{90}. It means the duration of the % 90 decrease of bacterias because of their death. The pollutant decay rate is equal to $2.3/T_{90}$.

k-ε turbulence formulation is used in turbulence submodel. The equations (13) and (14) have been used for kinetic energy and its rate of dissipation in the turbulence

$$\frac{\partial k}{\partial t}+u\frac{\partial k}{\partial x}+v\frac{\partial k}{\partial y}+w\frac{\partial k}{\partial z}= \frac{\partial}{\partial z}\left(\frac{v_z}{\sigma_k}\frac{\partial k}{\partial z}\right)+P+B-\varepsilon+ \frac{\partial}{\partial x}\left(D_x\frac{\partial k}{\partial x}\right)+\frac{\partial}{\partial y}\left(D_y\frac{\partial k}{\partial y}\right) \quad (13)$$

$$\frac{\partial \varepsilon}{\partial t}+u\frac{\partial \varepsilon}{\partial x}+v\frac{\partial \varepsilon}{\partial y}+w\frac{\partial \varepsilon}{\partial z}=\frac{\partial}{\partial z}\left(\frac{v_z}{\sigma_\varepsilon}\frac{\partial \varepsilon}{\partial z}\right)+ C_{1\varepsilon}\frac{\varepsilon}{k}(P+C_{3\varepsilon}B)-C_{2\varepsilon}\frac{\varepsilon^2}{k}+ \frac{\partial}{\partial x}\left(D_x\frac{\partial \varepsilon}{\partial x}\right)+\frac{\partial}{\partial y}\left(D_y\frac{\partial \varepsilon}{\partial y}\right) \quad (14)$$

Here, k is kinetic energy, ε is the rate of dissipation of kinetic energy; v_z is the vertical eddy viscosity; D_x, D_y are horizontal diffusion coefficients in x- and y -directions respectively; P is the stress production of the kinetic energy; B is the buoyancy production of the kinetic energy which is defined in the eqn. (15).

$$B=\frac{g}{\rho_0}\frac{v_z}{Pr}\frac{\partial \rho}{\partial z} \quad (15)$$

Where Pr is the turbulent Prandtl or Schmidt number. Experiments have shown that, the turbulent Prandtl or Schmidt number, varies slightly in a flow and from one flow to the other [10]. Therefore, it is considered as a constant, Pr = 0.7.

The stress production of the kinetic energy is defined in the eqn. (16).

$$P=v_h\left[2\left(\frac{\partial u}{\partial x}\right)^2+2\left(\frac{\partial v}{\partial y}\right)^2+\left(\frac{\partial u}{\partial y}+\frac{\partial v}{\partial x}\right)^2\right]+ v_z\left[\left(\frac{\partial u}{\partial z}\right)^2+\left(\frac{\partial v}{\partial z}\right)^2\right] \quad (16)$$

where v_h is the horizontal eddy viscosity and u and v are the horizontal water particle velocities in x- and y-directions respectively. The vertical eddy viscosity is calculated by:

$$v_z=C_\mu\frac{k^2}{\varepsilon} \quad (17)$$

The following universal empirical constants are used: C_μ = 0.09, σ_ε = *1.3,* $C_{1\varepsilon}$ = 1.44, $C_{2\varepsilon}$=1.92, $C_{3\varepsilon}$=1 if *B>0* (unstable stratification) and $C_{3\varepsilon}$ = 0.2 if *B<0* (stable stratification) [11]

The standard *k-*ε model assumes the local isotropy of the turbulence, where horizontal eddy viscosity is equal to the vertical eddy viscosity. If the horizontal motion has an intensity and length scale greater than the vertical motion, as in shallow water bodies, the standard single length scale, *k-*ε turbulence model underestimates the effective horizontal eddy viscosities. To account for large scale turbulence generated by the horizontal shear, horizontal eddy viscosity can be simulated by the Smagorinsky algebraic subgrid scale turbulence model [12].

There are four types of boundaries, namely; free surface, sea bed, open sea and coastal land boundaries.

3.2.1 Numerical Method

A composite finite difference-finite element method is applied to the goeverning equations. Finite difference method and finite element method are commonly used in various types of problems of computational fluid dynamics [13, 14, 15].

Equations are solved numerically by approximating the horizontal gradient terms using a staggered finite difference scheme as shown in Fig. (10) [8, 9].

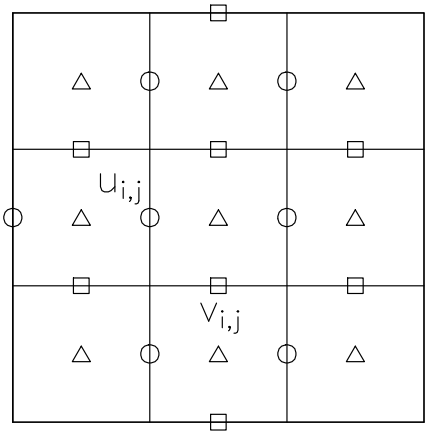

Fig 10: Staggered finite difference scheme in horizontal plane

In the vertical plane however, the Galerkin method of finite elements is utilized. Water depths are divided into the same number of layers following the bottom topography as shown in the Fig. (11). At all nodal points, the ratio of the length (thickness) of each element (layer) to the total depth is constant. To increase the vertical resolution, wherever necessary, grid clustering can be applied in the vertical plane. Grids can be concentrated near the bottom, surface, or intermediate layers. The mesh size may be varied in the horizontal plane [8, 9].

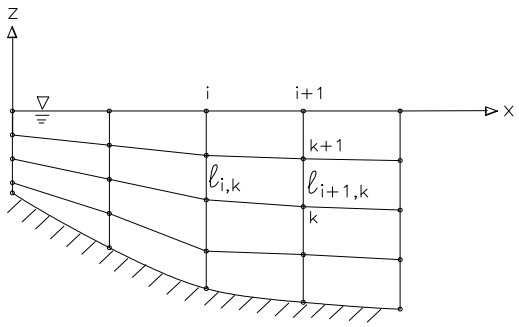

Fig. 11: Finite element scheme in vertical plane

By following the finite element approach, the values of velocities *u,* ***v****, w;* the turbulent eddy viscosities v_x, v_y, v_z; the temperature, *T;* the salinity *S;* the pollutant concentration *C*; the turbulent diffusivities D_x, D_y, D_z; the kinetic energy *k;* the rate of dissipation of kinetic energy ε; the pressure *p,* at any point over the flow depth are written in

terms of the discrete values of these variables at the vertical nodal points by using linear shape functions given in the eqn. (18) and (19) [8, 9].

$$\widetilde{G} = N_1 G_1^k + N_2 G_2^k \quad (18)$$

$$N_1 = \frac{z_2 - z}{l_k}; N_2 = \frac{z - z_1}{l_k}; l_k = z_2 - z_1 \quad (19)$$

Here $\widetilde{G}$ is the approximation or shape function, G is any of the variables, k is the element number, N_1 and N_2 are the interpolation functions, l_k is the length of the kth element, z_1 and z_2 are the beginning and end elevations of the element k, and z is the transformed variable that changes from z_1 to z_2 in an element.

The approximate expressions for variables are substituted into the governing equations and the residual errors *(R),* are minimized by using the Galerkin procedure [16, 17]. To increase the vertical resolution, wherever necessary, grid clustering can be applied in the vertical plane [18]. Grids can be concentrated near the bottom, surface, or intermediate layers.

After the application of the Galerkin method, any derivative terms with respect to horizontal co-ordinates appearing in the equations are replaced by their central finite difference approximations. The mesh size may be varied in the horizontal plane. The local element matrices for all elements on a vertical line are grouped together to form the global matrix equation for the unknown nodal time derivatives of the variables at a grid point on the horizontal plane. The sea bed and sea surface boundary conditions are taken into account, while building up the global matrices over the water depth [9]. The derivation of matrix elements can be found in the paper of Balas & Ozhan [8].

The system of non-linear equations are solved by the Crank-Nicholson method, which has second-order accuracy in time. To provide this accuracy, difference approximations are developed at the midpoint of the time step. The temporal first derivative is approximated at $(t + 1/2)$ and all other variables and derivatives at this time are determined by averaging the difference approximations at the beginning *(t)* and at the end $(t + 1)$ of the time increment. Resultant set of implicit equations are solved by an iterative method, which is controlled by underrelaxation. Underrelaxation is typically employed to make a non-convergent system convergent or to hasten convergence by dampening out the oscillations.

3.2.2 Application of HYDROTAM3

The wind induced current pattern after the 2 hours at the surface and at the bottom according to the wind velocity 10m/sec have been given in the Fig. 12 and Fig. 13. The wind blows from south.

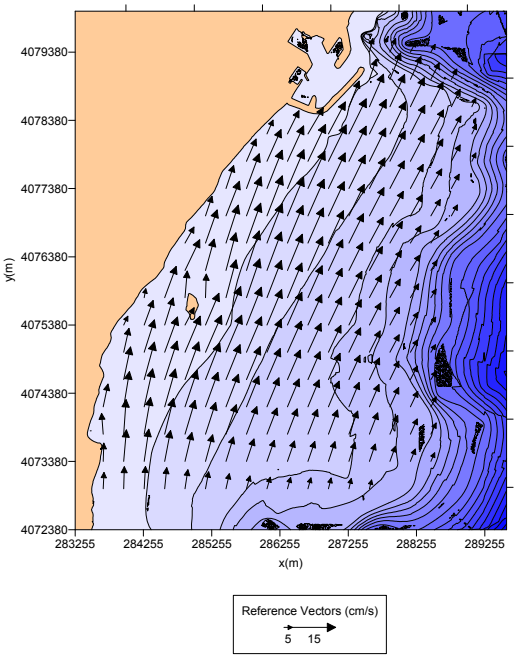

Fig. 12: Current velocity pattern at water surface after 2 hours

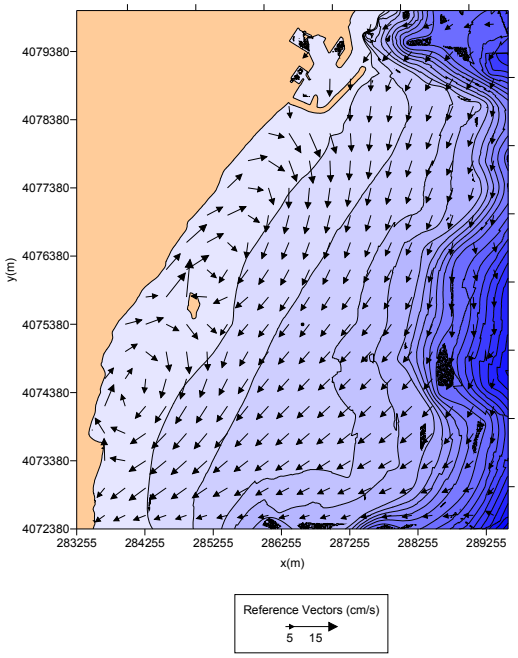

Fig. 13: Current velocity pattern at the bottom after 2 hours

The depth of the discharge point is 50m. It is shown as SO station point in the Fig. 14. The type of pipe material is HDPE. The minimum and maximum discharge flowrates are 280lt/sec and 4040lt/sec, respectively.

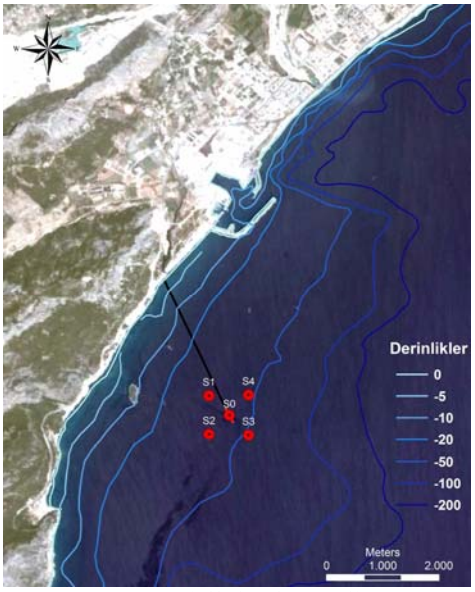

Fig. 14: Sea outfall discharge line

Pollutant concentration of the ambient sea is assumed to be zero initially. The initial concentration is 10^6 bac/ml. The concentration distribution at the surface and bottom after 2 hours have been presented in Fig. 15 and Fig. 16.

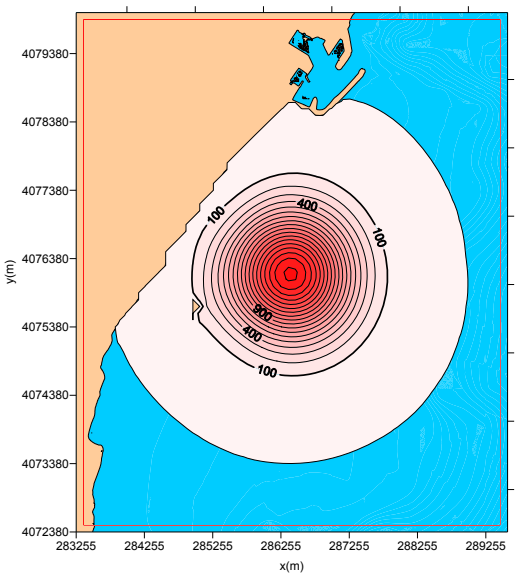

Fig. 15 : Concentration distribution at the surface after 2 hours

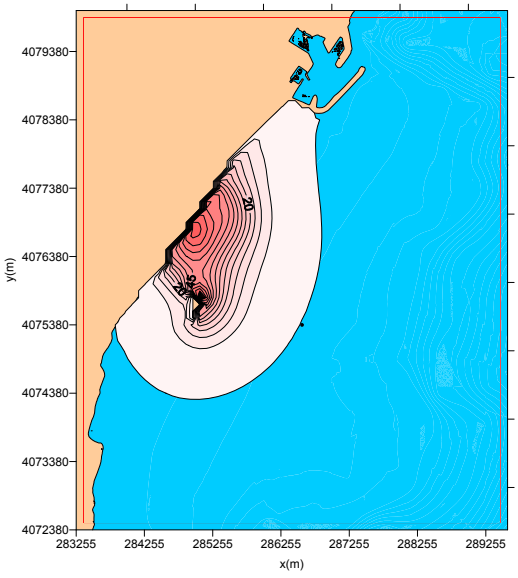

Fig. 16: Concentration distribution at the bottom after 2 hours

5 Conclusion

In this paper, the field studies for currents and wind measurements have been presented. The wave height distribution in the coastal area is shown. Current pattern and concentration distribution have been simulated numerically by HYDROTAM 3 which is a comprehensive baroclinic three-dimensional numerical model of transport processes in coastal areas. The numerical solution method is a composite finite element–finite difference method. The numerical model is a powerful design tool and can be implemented in a Decision Support System. After the final project report, environmental policy for the coastal area around Antalya Sea Outfall will be proposed and presented to the governmental and municipal authorites

Acknowledgement
This study is a part of the TUBITAK project called 'Investigation of Uncertainties in Predicting Bacterial Concentrations of Discharged Sewage from Deep Sea Outfalls When Submergence Occurs in Receiving Media'. It will be finalised in 2011. Thanks to the project, the effects of the sea outfall in Antalya has been considered in details and the obtained results can be used for the coastal management in Antalya.

References:

[1] Muhammmetoglu, A., Muhammet oglu, H., Topkaya, B., 'Monitoring and assessment of seawater quality around Antalya sea outfall', *Fresenius Environmental Bulletin*, Vol. 12, No 7, 2003, pp. 718-723

[2] Aral, N., Gonullu, M.T., Saral, A., 'Estimation of T90 and bacterial die-off rate values in the Antalya Bay of Turkey', *Journal of Environmental Science and Health- Part A Environmental Science and Engineering and Toxic and Hazaardous Substance Control*, Vol 30, No 10, 1995, pp. 2255- 2262

[3] Yalcin, O. B., Muhammmetoglu, A., 'Variations of bacterial inactivation of the discharged wastewater around Antalya sea outfall', *Fresenius Environmental Bulletin*, Vol. 13, No 11B, 2004, pp. 1225-1231

[4] TUBITAK Project Report 2: *Investigation of Uncertainties in Predicting Bacterial Concentrations of Discharged Sewage from Deep Sea Outfalls When Submergence Occurs in Receiving Media,* 2008

[5] http://www.map-of-turkey.co.uk/physical-map-of-turkey.htm

[6] Ozhan, E., Abdalla, S., *Wind and deep water wave atlas for Turkish coast,* Medcoast Publication, 1999

[7] US. Army Coastal Engineering Reserach, '*Shore Protection Manual*', Vol 1, 1984

[8] Balas, L., Ozhan, E., 'An implicit three-dimensional numerical model to simulate transport processes in coastal water bodies', *International Journal for Numerical Methods in Fluids*, Vol. 34, No 4, 2000, pp. 307-339

[9] Balas L., *Three-dimensional numerical modelling of transport processes in coastal water bodies*, PhD Thesis, The graduate school of Natural and Applied Sciences, Middle East Technical University, 1998

[10] Balas, L., Ozhan, E., 'Applications of a 3-D numerical model to circulation in coastal waters', *Coastal Engineering Journal*, Vol. 43, No 2, 2001, pp. 99-120

[11] Rodi W. *Turbulence models and their application in hydraulics*, IAHR Series (3rd edn). IAHR: Delft, The Netherlands, 1993.

[12] Mohammadi B, Pironneau O., *Analysis of the k-epsilon Turbulence Model,* John Wiley and Sons: London, UK, 1994.

[13] Nsom, B., Ndong, W., Ravelo, B., Modeling the Zero-Inertia, Horizontal Viscous Dam- Break Problem, *WSEAS Transactions on Fluid Mechanics,* Issue

2, Vol. 3, 2008, pp. 77-89

[14] Arico, C., Tucciarelli, T., Comparison of different 2nd order formulations for the solution of the 2D groundwater flow problem over irregular triangular mesh, *WSEAS Transactions on Fluid Mechanics,* Issue 2, Vol. 4, 2009, pp. 45-57

[15] Feng, Q., Zheng, B., Application of the Alternating Group Explicit Method for Convection- Diffusion Equations, *WSEAS Transactions on Mathematics,* Issue 3, Vol. 8, 2009, pp. 138-147

[16] Wardle AP, Hapoglu H. On the solution of models of binary and multicomponent packed distillation columns using orthogonal collocation on finite elements. *Chemical Engineering Research and Design, No: 72,* 1994, pp. 551-564.

[17] Karacan S, Cabbar Y, Alpbaz M, Hapoglu H. The steady state and dynamic analysis of packed distillation column based on partial differential approach. *Chemical Engineering and Processing, No: 37,* 1998, pp. 379-388

[18] Anderson AD, Tannehill JC, Pletcher RH. *Computational Fluid Mechanics and Heat Transfer.* Hemisphere Publishing Corporation: New York, USA, 1984.